High Fidelity Direct-Contrast Synthesis from Magnetic Resonance Fingerprinting in Diagnostic Imaging

Ke Wang[1], Mariya Doneva[2], Thomas Amthor[2], Vera C. Keil[3], Ekin Karasan[1], Fei Tan[4], Jonathan I. Tamir[1,5], Stella X. Yu[1,6], and Michael Lustig[1]
[1]Electrical Engineering and Computer Sciences, University of California, Berkeley, Berkeley, CA, United States, [2]Philips Research, Hamburg, Germany, [3]Universitätsklinikum Bonn, Bonn, Germany, [4]Bioengineering, UC Berkeley-UCSF, San Francisco, CA, United States, [5]Electrical and Computer Engineering, The University of Texas at Austin, Austin, TX, United States, [6]International Computer Science Institute, University of California, Berkeley, Berkeley, CA, United States

Synopsis

MR Fingerprinting is an emerging attractive candidate for multi-contrast imaging since it quickly generates reliable tissue parameter maps. However, contrast-weighted images generated from parameter maps often exhibit artifacts due to model and acquisition imperfections. Instead of direct modeling, we propose a supervised method to learn the mapping from MRF data directly to synthesized contrast-weighted images, *i.e.*, direct contrast synthesis (DCS). *In-vivo* experiments on both volunteers and patients show substantial improvements of our proposed method over previous DCS method and methods that derive synthetic images from parameter maps.

Introduction

Multi-contrast images generated from a single scan have the tremendous potential to streamline and shorten overall exam times. Magnetic Resonance Fingerprinting (MRF) is an emerging attractive candidate for multi-contrast imaging since it has been shown to generate reliable quantitative tissue parameter maps[1]. Although tissue quantification can be useful for diagnosis, clinicians typically prefer qualitative, contrast-weighted images. With MRF, these images can be synthesized from the quantitative maps by simulating the MRI physics (e.g. Synthetic MR[2]). Unfortunately, contrast-weighted images generated from parameter maps often exhibit artifacts due to model imperfections (e.g. flow, partial voluming). To overcome these limitations, deep learning has recently been used to map acquisition data directly to contrast-weighted images[3,4]. One approach used a pixel-wise network to fit the MRF time series to a qualitative contrast weighting at each pixel[3]. However, the method did not leverage the spatial and structural information. Here, we propose a spatial-convolutional supervised method for direct contrast synthesis (DCS). We employ a Generative Adversarial Network (GAN)[5] based framework, where MRF data can be used to synthesize T1-weighted, T2-weighted, and FLAIR images, which are common contrasts used in diagnostic imaging. Figure 1 summarizes the three different approaches of producing synthetic, multi-contrast images, out of which Figure 1.c is our proposed method. In-vivo experiments on both volunteers and patients show substantial improvements in image quality compared to previous DCS method and Synthetic MR from parameter maps.

Methods

Network Design:

We designed two GAN-based networks (**1-DCSNet** and **N-DCSNet**) for direct contrast synthesis from MRF data. Each network follows a standard conditional GAN framework with one generator G and one discriminator D (Figure 2). The generator is a U-Net[7] based convolutional network, which consists of one encoder and a single (**1-DCSNet**) or multiple decoders (**N-DCSNet**), while the discriminator is a Residual Network[8]. The output of the discriminator predicts whether the images are real (ground truth) or fake (synthesized images). The **N-DCSNet** uses a joint encoder with independent decoders to synthesize multi-contrast images, with the idea that contrast images share mutual information. All of the networks are trained with the learning rates 0.0001/0.0005 (Generator/Discriminator) for 100 epochs with batch size 4.

Loss function:

As shown in Figure 2, the loss function is a combination of the L_{pixel}, the l_1 loss between the synthesized the ground truth images, adversarial loss L_{adv}, as determined by the discriminator, and the perceptual loss L_{per}, which is calculated as the l_2 loss between the feature maps outputted by pre-trained VGG Net[9]. Therefore, the total loss can be written as

$$L_{total} = \lambda_1 L_{pixel} + \lambda_2 L_{per} + \lambda_3 L_{adv},$$

where $\lambda_i, i = 1, 2, 3$ are the weights for different losses. The addition of the adversarial and perceptual losses creates more realistic synthetic results. In order to make the training invariant to the input data scaling, we use a scaling invariant loss[10], where we multiply a scalar s to the output synthetic images $\hat{x}$ and use $s\hat{x}$ to compute the losses. s is easily computed by solving a least square problem:

$$\arg\min_s ||s\hat{x} - x||_2^2,$$

where x is the ground truth image. All of the networks were implemented in Pytorch[11] and trained using GeForce TITAN Xp GPUs.

Dataset and preprocessing:

All scans were performed with IRB approval and informed consent.

Volunteers: We scanned 21 volunteers between ages 29 to 61 years using a 1.5T Philips Ingenia scanner. 17 of the subjects were scanned twice, resulting in 38 datasets with 10 slices per sample. 36 samples are used as a training set while the other 2 are used as the test set.

Patients: A total of 30 patients (12 slices each) with different brain lesions (Parkinsons, Epilepsy, Tumor, Infarcts, etc.) were included in the study. All scans were conducted on a 3T Philips Achieva TX scanner. 26 out of 30 samples are used for training while the other 4 are used for testing.

For each sample in volunteers and patients, four MR examinations were conducted: T1w Spin Echo, T2w Turbo Spin Echo, FLAIR and a spiral MRF with variable flip angles (Captions in Figure 3 and 4 show the different sequence parameters for Volunteers and Patients). All the slices were normalized by the intensity of the white matter prior to training and testing. As the field strength and MRF parameters differed, separate networks were trained for the volunteers and patients' data.

Results

Figure 3 (Volunteers) and Figures 4 and 5 (Patients) display comparisons between different methods on three different synthesized contrasts in the test set. The high diagnostic quality of **1-DCSNet** and **N-DCSNet** contrast images from MRF data is eminent, showing more structural details, higher peak

signal-to-noise ratio (PSNR) and higher Structural Similarity Index (SSIM) compared to our implementation of PixelNet and Synthetic MR from parameter maps, even in the presence of large off-resonance artifacts.

Discussion and Conclusion

Our proposed direct contrast synthesis method demonstrates that multi-contrast MR images can be synthesized from a single MRF acquisition with sharper contrast, minimal artifacts, and a high PSNR on both volunteers and patients. Additionally, **N-DCSNet** also implicitly learns some spiral deblurring. By directly training a network to generate contrast images from MRF, our method does not use any model-based simulation steps and therefore can also avoid any reconstruction errors due to simulation.

Acknowledgements

No acknowledgement found.

References

1. Ma, D., Gulani, V., Seiberlich, N., Liu, K., Sunshine, J. L., Duerk, J. L., & Griswold, M. A. (2013). Magnetic resonance fingerprinting. Nature, 495(7440), 187.

2. Hagiwara, A., Warntjes, M., Hori, M., Andica, C., Nakazawa, M., Kumamaru, K. K., ... & Aoki, S. (2017). SyMRI of the brain: rapid quantification of relaxation rates and proton density, with synthetic MRI, automatic brain segmentation, and myelin measurement. Investigative radiology, 52(10), 647.

3. Patrick Virtue, Mariya Doneva, Jonathan I. Tamir, Peter Koken, Stella X. Yu, and Michael Lustig.Direct contrast synthesis for magnetic resonance fingerprinting. In Proc. Intl. Soc. Mag. Reson. Med, 2018

4. Guanhua Wang, Enhao Gong, Suchandrima Banerjee, Huijun Chen, John Pauly, Greg Zaharchuk. OneforAll: Improving the Quality of Multi-contrast Synthesized MRI Using a Multi-Task Generative Model. In Proc. Intl. Soc. Mag. Reson. Med, 2019

5. Goodfellow, I., Pouget-Abadie, J., Mirza, M., Xu, B., Warde-Farley, D., Ozair, S., ... & Bengio, Y. (2014). Generative adversarial nets. In Advances in neural information processing systems (pp. 2672-2680).

6. Hennig, J., Weigel, M., & Scheffler, K. (2004). Calculation of flip angles for echo trains with predefined amplitudes with the extended phase graph (EPG)-algorithm: principles and applications to hyperecho and TRAPS sequences. Magnetic Resonance in Medicine: An Official Journal of the International Society for Magnetic Resonance in Medicine, 51(1), 68-80.

7. Ronneberger, O., Fischer, P., & Brox, T. (2015, October). U-net: Convolutional networks for biomedical image segmentation. In International Conference on Medical image computing and computer-assisted intervention (pp. 234-241). Springer, Cham.

8. He, K., Zhang, X., Ren, S., & Sun, J. (2016). Deep residual learning for image recognition. In Proceedings of the IEEE conference on computer vision and pattern recognition (pp. 770-778).

9. Simonyan, K., & Zisserman, A. (2014). Very deep convolutional networks for large-scale image recognition. arXiv preprint arXiv:1409.1556.

10. Eigen, D., & Fergus, R. (2015). Predicting depth, surface normals and semantic labels with a common multi-scale convolutional architecture. In Proceedings of the IEEE international conference on computer vision (pp. 2650-2658).

11. Paszke, A., Gross, S., Chintala, S., Chanan, G., Yang, E., DeVito, Z., ... & Lerer, A. (2017). Automatic differentiation in pytorch.

Figures

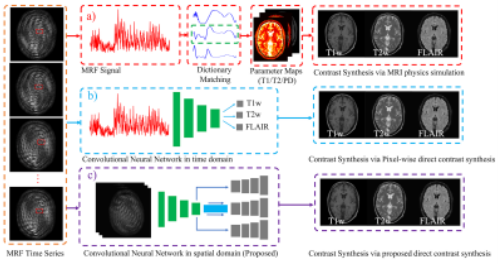

Figure 1. Three possible pipelines for synthetic multi-contrast images: a) through dictionary matching and sequence simulation (Bloch simulation, Extended Phase Graph Algorithm[6]). b) pixel-wise time-domain convolutional neural network[3]. c) our proposed spatial-convolution GAN-based direct contrast synthesis method.

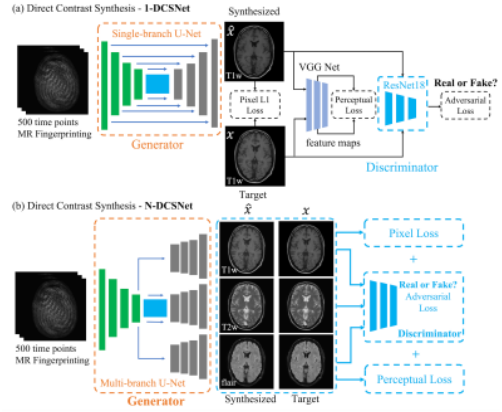

Figure 2. Network architectures of the proposed method. a) the 1-DCSNet: A conventional U-Net composes the generator where the input is 500-time points MRF data and the output is one synthesized contrast-weighted image. Pre-trained VGG 16[9] and ResNet 18[8] (the discriminator) are used as the backbone to compute the perceptual loss and the adversarial loss. b) the N-DCSNet: A modified Multi-decoders U-Net is used for the generator where the outputs are multiple contrast-weighted images. Different contrast-weighted images are concatenated as the input of VGG 16 and the discriminator.

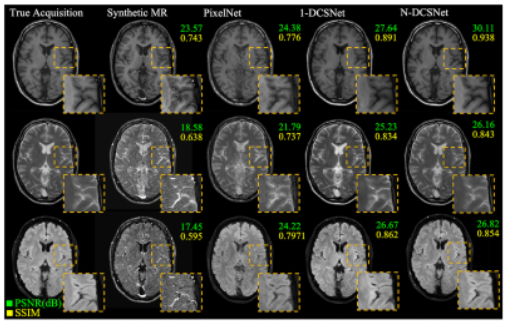

Figure 3. Comparison between different methods on three different synthesized contrasts for Volunteer data. Zoom-in details are displayed on the side of each image, which shows a better cortex to white matter contrast and improved SNR in 1-DCSNet and N-DCSNet. Sequence parameters for the tru scan: 1) T1w SE with TE = 15ms, TR = 450ms, FA = 69; 2) T2w TSE with TE = 110ms, TR = 1990-2215 ms, ETL=16, FA = 90; 3) FLAIR with TE = 120ms, TR = 8500ms, TI=2500ms,ETL=41, FA = 90. 4) MRF spoiled gradient each (FISP) sequence with 500 time points, constant TE = 3.3ms and TR = 20ms with variable flip angles.

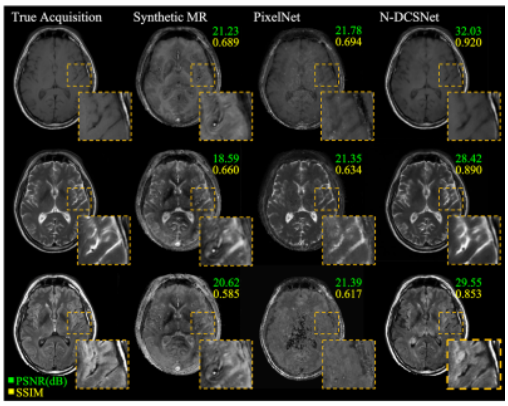

Figure 4. Comparison between different methods on three different contrasts for Patients data. This patient has been diagnosed with Parkinson disease. Some white matter lesions can be seen in the true acquisition. Zoom-in details show better white matter contrast and improved SNR in N-DCSNet. Scanning parameters: 1)T1w SE: TE = 13.4 ms, TR=520ms, FA = 90; 2) T2w TSE: TE = 80ms, TR = 1758 ms, ETL=15, FA = 90; 3) FLAIR: TE = 140ms, TR = 12000ms, TI=2850ms,ETL=40, FA = 90. 4) MRF spoiled gradient each (FISP) sequence with 500 time points, constant TE = 4ms and TR = 20ms with variable flip angles.

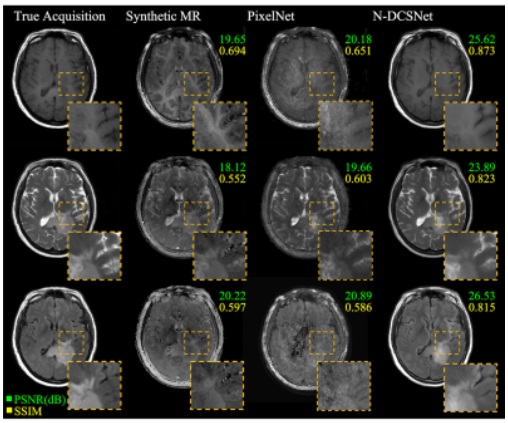

Figure 5. Comparison between different methods on three different synthesized contrasts for Patients data. This patient has been diagnosed with a brain tumor, where massive tumor can be seen on the images. Zoom-in details show sharper structures and improved SNR in N-DCSNet. Without training on a large tumor datasets, N-DCSNet can still recover the structure of the tumor, but with a soft contrast and blur edges compared to the true acquisition. The scanning parameters are the same as in Figure 4.